

Direct Probing of a Polymer Electrolyte/Luminescent Conjugated Polymer Mixed Ionic/Electronic Conductor

Yufeng Hu and Jun Gao*

Department of Physics, Engineering Physics and Astronomy, Queen's University, Kingston, Ontario K7L 3N6, Canada

Received October 25, 2009; E-mail: jungao@physics.queensu.ca

The composite of a polymer electrolyte and a luminescent conjugated polymer is a mixed ionic/electronic conductor (MIEC) first studied in the so-called polymer light-emitting electrochemical cell (LEC), which employs a polymer MIEC thin film sandwiched between two electrodes.¹ The application of a sufficiently large voltage bias leads to electroluminescence from the luminescent polymer as the injected electronic charges undergo radiative recombination. The fundamental operating mechanism of an LEC was thought to be *in situ* electrochemical doping of the luminescent polymer followed by the formation of a dynamic, light-emitting p–n junction.^{2–6} This LEC model is consistent with the observation of localized electroluminescence in planar cells with micrometer-sized interelectrode gaps.^{1,7}

Early LEC research, however, was mainly conducted on thin sandwich cells that can be efficient light emitters but do not allow direct observation of the dynamic doping processes.^{8–15} The lack of direct evidence for doping has led to the proposal of an alternative LEC model, which attributes the unique LEC device characteristics to “ionic space charge” effects without invoking electrochemical doping.¹⁶ Much has changed since the demonstration of planar LECs with millimeter-sized interelectrode spacing, which were turned on by applying a voltage bias of several hundred volts to overcome the enormous series resistance of the undoped polymer film.^{17,18} The extremely large and fully exposed interelectrode gap allows for time-lapse fluorescence imaging with high temporal and spatial resolution. For the first time the dynamic p- and n-doping as well as the junction formation processes were captured on camera, providing conclusive evidence in support of the original LEC model.^{19–22}

Here we show it is possible to induce strong electrochemical doping and electroluminescence by biasing a pair of sharp tungsten probes in direct contact with the polymer MIEC film, *without any predeposited electrodes*. We discuss the findings and the potential applications of this new technique in the study of MIEC films.

Figure 1 shows the time-lapse images of an MIEC film under ultraviolet (UV) illumination. The MIEC film contains poly[5-(2-ethylhexyloxy)-2-methoxy-1, 4-phenylene vinylene] (MEH-PPV), a red-emitting luminescent conjugated polymer. The MIEC also contains polyethylene oxide (PEO), an ion-solvating/conducting polymer, and cesium perchlorate. Two tungsten probes with a tip radius of 10 μm were brought into contact with the polymer film at ~4.8 mm apart. This probe distance was large enough for imaging with a digital SLR camera without additional optical magnification. Upon the application of a 400 V bias, darkened profiles could be seen to emerge from the probe tips and to grow in size with time (Figure 1b–d). The darkening of the polymer film under UV illumination indicates fluorescence quenching and is caused by the electrochemical doping of the luminescent polymer.²³ Unlike in planar LECs with long, straight electrodes, the point-like metal–polymer contact here gives rise to an n-doping profile that is nearly

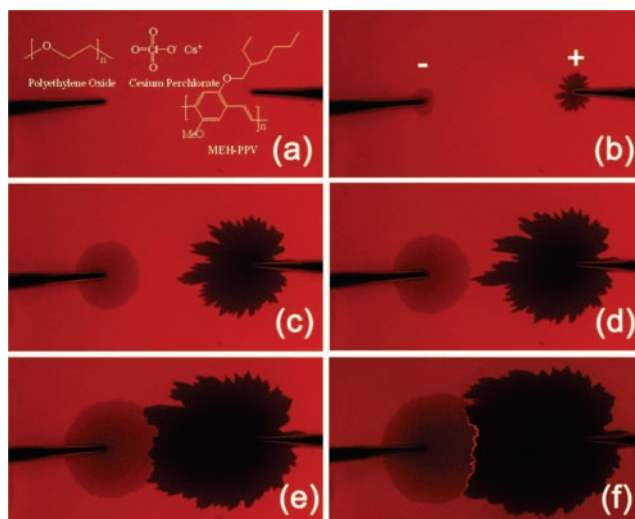


Figure 1. MEH-PPV:PEO:CsClO₄ film in contact with two tungsten probes at 4.8 mm apart. The film is at 330 K and under UV illumination. Time elapsed since a 400 V bias was applied: (a) no bias, (b) 10 s, (c) 90 s, (d) 120 s, (e) 220 s, and (f) 270 s.

circular and extremely smooth at the doping front. The p-doping front is quite uneven although the overall shape of the p-doped region also resembles a circle. The p- and n-doped regions eventually make full contact between the tips to form a p–n junction (Figure 1e), and electroluminescence can be observed in the junction area when it is stronger than the background fluorescence (Figure 1f).

The polarity of the voltage bias was subsequently reversed. Initially the doping profiles established under “forward bias” were largely intact. A striking observation is the appearance of dark, tree-like p-doping profiles in the previously n-doped region on the left (Figure 2a–b). These doping patterns resemble fractals as they possess self-similarity. At the right, a new, circular n-doping pattern emerges. The new n-doping reverses the strong fluorescence quenching induced by the previous p-doping process. The degree of fluorescence quenching in areas not affected by new p- and n-doping also decreased over time, which indicates spontaneous doping relaxation (Figure 2c–d). Eventually the new p- and n-doped regions made contact and electroluminescence was again observed (Figure 2e–f). However, the new light-emitting p–n junction formed was not continuous due to the highly branched nature of p-doping propagation.

Electrochemical p-doping of a conjugated polymer involved the oxidation of the polymer and the insertion of compensating anions near the doping site.²⁴ The dramatically different p-doping patterns observed under “forward” and “reverse” bias suggests differing reaction kinetics. In a fresh MIEC film, the p-doping reaction is

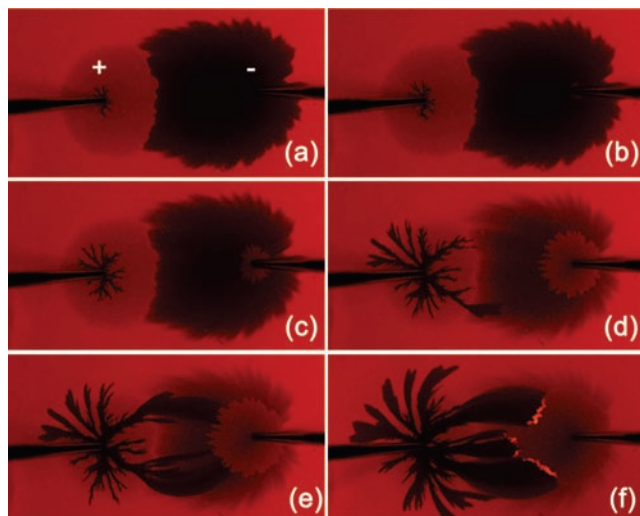


Figure 2. The same MEH-PPV:PEO:CsClO₄ film as in Figure 1 upon bias polarity reversal. Time elapsed since voltage polarity change (a) 30 s, (b) 50 s, (c) 100 s, (d) 200 s, (e) 280 s, and (f) 380 s.

likely rate-limited by electrode kinetics, i.e., the rate of electron transfer across the interface between doped and undoped regions. When the voltage bias is reversed, the polymer film near the positive tip is nearly devoid of the anions necessary for p-doping due to previous n-doping. As a result, mass transport becomes the rate-determining factor. The transport of anions to the doping site is likely due to a combination of diffusion and drift. Assuming the motion of anions has sufficient randomness (random walk) and comes to a stop at the doping front, then the diffusion-limited-aggregation (DLA) model predicts a highly branched and fractal growth pattern similar to that shown in Figure 2.²⁵ The fractal growth pattern is widely observed in electrodeposition, and electropolymerization reactions.^{26–30} Here we observe the first example involving electrochemical doping and a luminescent conjugated polymer. We also note that once the tips of p-doping crosses into the old p-doped region, as seen in Figure 2d–e, the p-doping speeds up dramatically and no longer branches out. This is expected as ample anions become available and the p-doping growth is no longer mass transport-limited. n-Doping, on the other hand, does not display any fractal growth behavior even in the previously p-doped region, as seen in Figure 2. The cause of this asymmetry between p- and n-doping is under investigation. However, the fractal p-doping growth is unlikely caused by any irreversible damage induced by the previous n-doping because the photoluminescence of the n-doped region appears to completely recover in areas not affected by p-doping (Figure 2).

The obvious advantages of the direct probing technique demonstrated here are its simplicity and versatility. The probe location and probe distance can be easily changed. The point-like contact

also possesses all the advantages of a microelectrode and is ideally suited for voltammetry studies. The probing was carried out under vacuum in a micromanipulated cryogenic probe station. This allows a desired doping profile to be established at high temperature and subsequently frozen by cooling to below the glass transition temperature of the polymer electrolyte.³¹ The probes can then be manipulated to various locations to map the electrical potential and conductivity of a frozen polymer p–n junction.

Acknowledgment. Jun Gao thanks American Dye Source, Inc. for providing the luminescent polymer used in this research. This project is supported by the Natural Sciences and Engineering Research Council (NSERC) of Canada.

Supporting Information Available: Experimental details (S1); Time evolution of device current under forward and reverse bias (S2). This material is available free of charge via the Internet at <http://pubs.acs.org>.

References

- (1) Pei, Q. B.; Yu, G.; Zhang, C.; Yang, Y.; Heeger, A. J. *Science* **1995**, *269*, 1086–1088.
- (2) Pei, Q. B.; Yang, Y.; Yu, G.; Zhang, C.; Heeger, A. J. *J. Am. Chem. Soc.* **1996**, *118*, 3922–3929.
- (3) Sun, Q. J.; Li, Y. F.; Pei, Q. B. *J. Display Technol.* **2007**, *3*, 211–224.
- (4) Edman, L. *Electrochim. Acta* **2005**, *50*, 3878–3885.
- (5) Shao, Y.; Bazan, G. C.; Heeger, A. J. *Adv. Mater.* **2007**, *19*, 365–.
- (6) Pei, Q.; Heeger, A. J. *Nat. Mater.* **2008**, *7*, 167–167.
- (7) Dick, D. J.; Heeger, A. J.; Yang, Y.; Pei, Q. B. *Adv. Mater.* **1996**, *8*, 985–987.
- (8) Pei, Q.; Yang, Y.; Yu, G.; Cao, Y.; Heeger, A. J. *Synth. Met.* **1997**, *85*, 1229–1232.
- (9) Yang, Y.; Pei, Q. B. *J. Appl. Phys.* **1997**, *81*, 3294–3298.
- (10) Yang, Y.; Pei, Q. B. *Appl. Phys. Lett.* **1997**, *70*, 1926–1928.
- (11) Yu, G.; Yang, Y.; Cao, Y.; Pei, Q.; Zhang, C.; Heeger, A. J. *Chem. Phys. Lett.* **1996**, *259*, 465–468.
- (12) Yang, Y.; Pei, Q. B. *Appl. Phys. Lett.* **1996**, *68*, 2708–2710.
- (13) Cao, Y.; Pei, Q. B.; Andersson, M. R.; Yu, G.; Heeger, A. J. *J. Electrochem. Soc.* **1997**, *144*, L317–L320.
- (14) Li, Y. F.; Gao, J.; Yu, G.; Cao, Y.; Heeger, A. J. *Chem. Phys. Lett.* **1998**, *287*, 83–88.
- (15) Tasch, S.; Holzer, L.; Wenzl, F. P.; Gao, J.; Winkler, B.; Dai, L.; Mau, A. W. H.; Sotgiu, R.; Sampietro, M.; Scherf, U.; Mullen, K.; Heeger, A. J.; Leising, G. *Synth. Met.* **1999**, *102*, 1046–1049.
- (16) deMello, J. C.; Tessler, N.; Graham, S. C.; Friend, R. H. *Phys. Rev. B* **1998**, *57*, 12951–12963.
- (17) Gao, J.; Dane, J. *Appl. Phys. Lett.* **2003**, *83*, 3027–3029.
- (18) Gao, J.; Dane, J. *Appl. Phys. Lett.* **2004**, *84*, 2778–2780.
- (19) Hu, Y.; Tracy, C.; Gao, J. *Appl. Phys. Lett.* **2006**, *88*, 123507.
- (20) Hu, Y. F.; Gao, J. *Appl. Phys. Lett.* **2006**, *89*.
- (21) Shin, J. H.; Dzwilewski, A.; Iwasiewicz, A.; Xiao, S.; Fransson, A.; Anka, G. N.; Edman, L. *Appl. Phys. Lett.* **2006**, *89*.
- (22) Shin, J. H.; Robinson, N. D.; Xiao, S.; Edman, L. *Adv. Funct. Mater.* **2007**, *17*, 1807–1813.
- (23) Holt, A. L.; Leger, J. M.; Carter, S. A. *J. Chem. Phys.* **2005**, *123*, 044704.
- (24) Scrosati, B. In *Solid State Electrochemistry*; Bruce, P. G., Ed.; Cambridge University Press: 1995; p 248.
- (25) Sander, L. M. *Nature* **1986**, *322*, 789–793.
- (26) Matsushita, M.; Sano, M.; Hayakawa, Y.; Honjo, H.; Sawada, Y. *Phys. Rev. Lett.* **1984**, *53*, 286–289.
- (27) Ligon, W. V. *J. Chem. Educ.* **1987**, *64*, 1053–1053.
- (28) Fujii, M.; Yoshino, K. *Jpn. J. Appl. Phys., Part 2* **1988**, *27*, L457–L460.
- (29) Kaufman, J. H.; Nazzari, A. I.; Melroy, O. R.; Kapitulin, A. *Phys. Rev. B* **1987**, *35*, 1881–1890.
- (30) Fujii, M.; Arai, K.; Yoshino, K. *Synth. Met.* **1993**, *55*, 1159–1164.
- (31) Gao, J.; Yu, G.; Heeger, A. J. *Appl. Phys. Lett.* **1997**, *71*, 1293–95.

JA908962B